EXPERIMENTAL AND COMPUTATIONAL INVESTIGATIONS OF FLOW BY-PASS IN A 37-ELEMENT CANDU FUEL BUNDLE IN A CREPT PRESSURE TUBE

M.H.A. Piro[a,*], M. Bruschewski[b], D. Freudenhammer[c], C. Azih[a], B. Tensuda[a,d], F. Wassermann[c], S. Grundmann[e], S.J. Kim[f], M. Christon[g], M. Berndt[h] and C. Tropea[c]

[a] *Fuel and Fuel Channel Safety Branch, Canadian Nuclear Laboratories, Chalk River, ON, Canada*
[b] *Institute of Gas Turbines and Aerospace Propulsion, Technische Universität Darmstadt, Darmstadt, Germany*
[c] *Institute of Fluid Mechanics and Aerodynamics, Center of Smart Interfaces, Technische Universität Darmstadt, Darmstadt, Germany*
[d] *University of Toronto Institute for Aerospace Studies, University of Toronto, Toronto, Canada*
[e] *Institute of Fluid Mechanics, University of Rostock, Rostock, Germany*
[f] *Mechanical and Thermal Engineering, Los Alamos National Laboratory, Los Alamos, NM, USA*
[g] *Computational Sciences International, Los Alamos, NM, USA*
[h] *Computer, Computational and Statistical Sciences, Los Alamos National Laboratory, Los Alamos, NM, USA*

* Corresponding author: +1 613 584 8811 x 42530; markus.piro@cnl.ca.

ABSTRACT

The current work presents investigations of fluid flow through a 37-element CANDU nuclear fuel bundle residing within a deformed pressure tube. This scenario simulates the long-term effects of aging, whereby the pressure tube may experience up to 6% diametral creep, resulting in appreciable flow by-pass and the concomitant increase in fuel temperature due to local undercooling. This work examines in high spatial detail the three-dimensional, three-component fluid velocity field through the fuel channel. A companion paper is dedicated to the experimental component of this work, which is based on Magnetic Resonance Velocimetry. In the present paper, computational fluid dynamic simulations have been performed with HYDRA-TH using an implicit large eddy simulation to predict turbulent flow behaviour. Together, an improved understanding has been gained in quantifying flow by-pass, the evolution of geometry-induced inter-subchannel mixing, the local effects of obstructing debris on the local flow field, and various turbulent effects, such as recirculation, swirl and separated flow. These capabilities are not possible with conventional experimental techniques or thermal-hydraulic codes. The overall goal of this work is to continue developing experimental and computational capabilities for continued investigations to support nuclear reactor performance and safety.

1 INTRODUCTION

Unlike Light Water Reactors, CANDU reactors have horizontally configured fuel channels that may experience appreciable creep over the lifetime of the channel (i.e., up to ≈6% in diameter). As a consequence of diametral creep, the space on the top of the fuel channel increases and the coolant distribution, following the path of least resistance, flows more above the bundle in comparison to a normal undeformed pressure tube. Hence, the coolant flow through the inner regions of the bundle is reduced, which in turn increases the local temperature field. Having an understanding of internal flow conditions is therefore important in quantifying the coolability of individual fuel elements within the fuel bundle.

Established experimental methods are ineffective at accurately measuring fluid velocity within a fuel bundle due to physical obstructions or lack of optical access into the flow regime. Also, while conventional thermal-hydraulic codes are effective at system level or bundle level analyses, they rely heavily on empirical correlations that are not universal in nature and are unable to capture local effects with high spatial fidelity.

This work examines the three-dimensional, three-component (3D3C) fluid velocity field with Magnetic Resonance Velocimetry (MRV) measurements and Computational Fluid Dynamics (CFD) simulations. In brief, MRV is able to non-intrusively measure 3D3C fluid velocity without requiring optical access to the measurement volume, and without injection of tracer particles into the flow field. A companion paper is dedicated to describing the MRV technique and the associated measurements (Bruschewski et al. 2016). In the present study, CFD simulations were performed to investigate detailed time-dependent turbulent behavior of the flow through the fuel channel for both scenarios involving a normal and crept pressure tube. Due to the requirement of using non-metallic materials (i.e., polymers) in an MRI, the flow conditions that were analyzed – specifically temperature, pressure and flow rate – were not the same as in-reactor conditions. Nevertheless, this work is intended to gain insight into the effects of flow by-pass while further developing experimental and computational capabilities to provide high resolution velocity data that cannot be provided by conventional techniques.

2 BACKGROUND

This paper describes the third experimental and computational campaign in investigating fluid flow through a CANDU fuel channel. The first investigation was a proof-of-concept that employed a simplified 8-element fuel bundle replica produced with polyamide material via additive manufacturing (Piro et al. 2016a). The second investigation used a 37-element bundle replica sitting in a pressure tube that was geometrically consistent with what is used in industry (Piro et al. 2016b). The third investigation, which is described herein, examines flow through a 37-element bundle sitting on the bottom of a pressure tube that is 6% greater in diameter than a standard pressure tube. The intention is to maintain consistency with all other parameters in the current investigation with respect to the previous campaign to isolate the comparison of flow characteristics due to increased pressure tube diameter resulting in flow by-pass.

A standard 37-element CANDU fuel bundle is shown in Figure 1a with salient features identified. In this design, fuel elements are mated together with Zircaloy-4 end plates to maintain spacing between adjacent elements. Spacer pads are located in the mid-length of the bundle and prevent direct contact between elements. Bearing pads are appended to the outer ring of fuel elements to provide spacing from the adjacent pressure tube wall, as shown in Figure 1b, which is intended to provide a pathway for water to travel for cooling purposes. The fuel bundle, pressure tube and calandria tube collectively constitute the fuel channel.

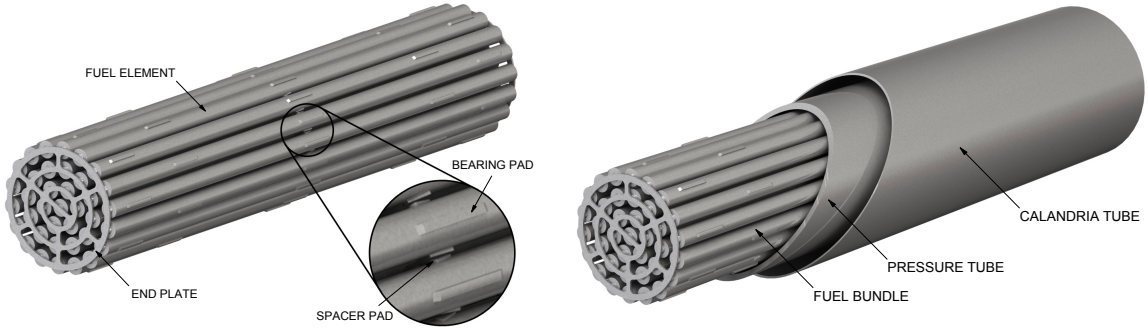

Figure 1. a) A 37-element CANDU fuel bundle is shown with salient features identified. b) A 37-element CANDU fuel bundle is shown sitting within a pressure tube, which is housed in a Calandria tube [Piro et al. 2016a].

Due to the horizontal configuration of fuel channels in the CANDU design, a fuel bundle will sit on the bottom of a pressure tube. Over time, the pressure tube may experience diametral creep due to the large pressure differential between the inside and outside of the pressure tube (i.e., ≈10 MPa), which is accelerated by neutron fluence induced damage mechnisms. For the case of a diametrically crept pressure tube, the volumetric region on the top of the fuel channel increases and the coolant, following the path of least resistance, will flow preferentially above the bundle (Piro et al. 2016a).

Hence, coolant mass flow rate required to keep the inner fuel elements will by-pass these inner regions of the bundle, which in turn will increase the local temperature field. This phenomenon is commonly referred to as flow by-pass. Figure 2 illustrates the difference between the cross-section of a bundle sitting in a normal and a crept pressure tube. Figure 2b highlights the large open region on the top of the fuel channel that gives rise to flow by-pass.

All pressure tubes in operating CANDU reactors experience some diametral creep over sufficient periods of time. The design end-of-life limit of pressure tube diametral creep is 6% in some plants, and as long as sufficient bundle cooling can be demonstrated, higher diamteral creep can be established as end-of-life limit without the reactor being de-rated in order to satisfy safety concerns, which has a direct impact on performance. This limit is currently considered conservative (Holt 2008). Therefore, there is a direct financial incentive for industry to better understand this phenomenon to provide a technical basis for justifying a larger end-of-life limit for diametral creep. Thus, the work described herein serves two purposes: 1) to quantify the effects of flow by-pass to support engineering safety analyses of CANDU fuel channels; and 2) to further develop state-of-the-art experimental and computational fluid dynamic capabilities to broadly support nuclear reactor performance and safety.

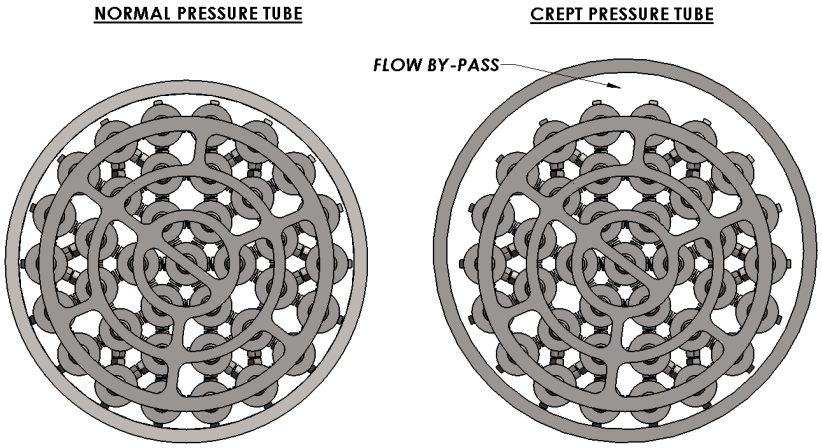

Figure 2. An end view comparison of a 37-element CANDU fuel bundle sitting in a normal pressure tube (left) and a 6% crept pressure tube (right).

3 EXPERIMENTAL CONSIDERATIONS

The experimental setup, used for the acquisition of the MRV measurements, is visualized in Figure 3. The setup is a 1:1 scale model of a 37-element CANDU fuel bundle, made from Polyamide in a selective laser sintering production process (fuel bundle and diffuser) and perspex (pressure tube replica). The 37 elements of the fuel bundle are positioned by endplates with spacer pads between the single fuel elements and appendages. The fuel bundle was manufactured in two parts and mated together to a total length of 495 mm. To prevent the fuel bundle replica from moving during the experiment, since the polyamid material has a relatively low specific gravity, it was mounted to the rig from the rear.

The fuel bundle replica is connected to a flow supply system via PVC hoses. The flow enters the system from the left through a diffuser section, which expands the cross section from the inlet hose to the cross section of the larger pressure tube. Grids inside the diffuser prevent flow separation. A nozzle at the end of the system reduces the diameter of the fuel channel to the diameter of the return hose. The measurement region covers nearly the entire fuel channel containing one bundle.

In contrast to the experimental setup previously presented by Piro et al. (2016b), the pressure tube is increased in size by 6% to 110 mm inner diameter (versus ≈103 mm before) to simulate the geometry of a crept pressure tube. The fuel bundle remains the same size with a diameter of ≈102 mm. A cross

section of the pressure tube and fuel bundle is visualized in Figure 3 (top left). Due to the smaller diameter of the fuel bundle compared to the pressure tube, a flow by-pass region is created in the upper part of the pressure tube (shaded red), with a maximum height of ≈10 mm.
The working fluid is de-ionized water with a copper sulfate contrast agent at a concentration of 1 g/L. The contrast agent enhances the signal magnitude, which speeds up the measurements; however, it does not significantly alter the fluid properties of the water. The water temperature was held constant at 20.5 °C. A constant volumetric flow rate of 60 L/min was set using the flow supply system. This flow rate is much lower than what is typically experienced in-reactor, which is typically about 1200 L/min. Although the flow conditions considered in these analyses are not representative of in-reactor conditions – specifically, lower temperature, hydrostatic pressure and mass flow rate – the intent of this work is to gain confidence in the combined experimental and computational approach, which will be extended to in-reactor conditions in future work.

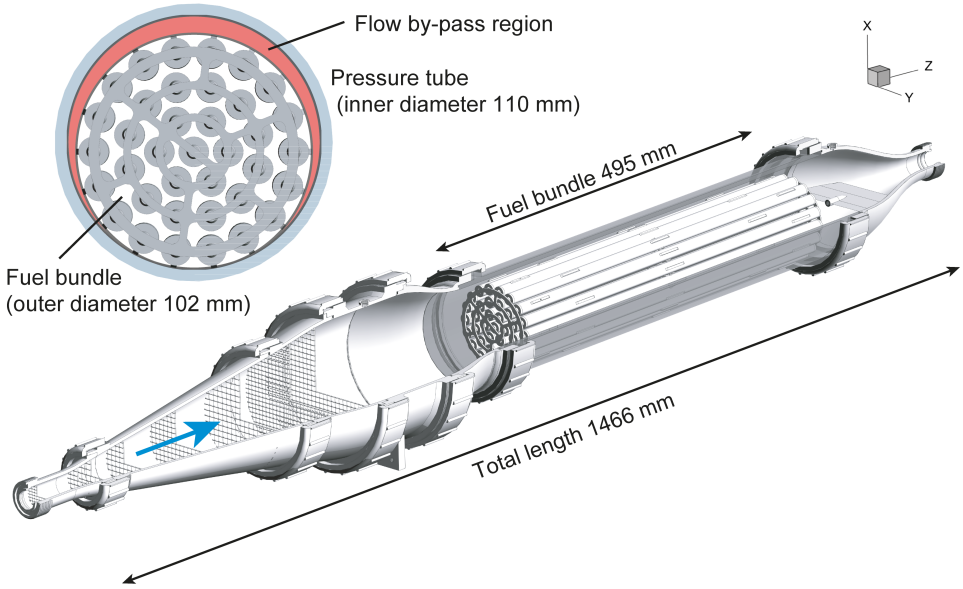

Figure 3. Schematic of the experimental setup used for the MRV measurements. The setup is made from Perspex and Polyamide through a selective laser sintering production process. Figure copied from Bruschewski et al. (2016).

MRV measurements were carried out on a MAGNETOM Prisma MRI system (Siemens Healthcare, Erlangen, Germany) at the Medical Center Freiburg. A velocity-encoded gradient echo FLASH (fast low angle shot) sequence was chosen for the measurements. The velocity sensitivity (VENC), describing the maximum measurable velocities, was set to 0.4 m/s.

Due to the large volume of the region of interest (≈550 mm in length and ≈110 mm in diameter), the measurement volume was divided into five separate, overlapping Field-of-Views (FOV). Each FOV comprised of a 160 x 180 x 320 data matrix with a spatial resolution of 0.78 mm in each direction. This cubic volume is commonly referred to as a "voxel". Each FOV was measured twice with a constant flow rate (flow-on scan), in order to improve the measurement uncertainty of the MRV-data. One flow-off scan (i.e., a measurement with the same parameters yet without flow) was carried out for each FOV. Apparent flow velocities within the flow-off scan originate from systematic errors (i.e., induced eddy currents) and are subtracted from the flow-on scans to improve the accuracy of the measurement. Data acquisition for each FOV (two flow-on & one flow-off scan) took 47 minutes, adding up to a total data acquisition time of just less than 4 hours. More detailed information regarding the experimental considerations can be found in the companion paper Bruschewski et al. (2016).

4 COMPUTATIONAL CONSIDERATIONS

The complex intricacies and orientations in the surfaces that bound the flow through the CANDU fuel bundle increase the complexity of the flow. For instance, the front and rear end plates induce separation and rotation, the skewed spacer pads induce swirl and the combination of various effects lead to inter-subchannel mixing. Therefore, the present simulations require sufficient spatial resolution to facilitate detailed comparison to the MRV measurements outlined in the previous section and described in Bruschewski et al. (2016).

Several previously published articles related to fluid flow through a CANDU fuel bundle have independently demonstrated that turbulence closure models based on the Reynolds Averaged Navier-Stokes (RANS) equations are reasonable for this particular flow problem, but generally do not perform as well as Large Eddy Simulatoin (LES). These claims have also been supported by experimental measurements (Piro et al. 2016a; Bhattacharya et al. 2012; Abbasian et al. 2009). Furthermore, RANS models under-predict inter-subchannel mixing in a fuel bundle due to its inherent inability to capture turbulent anisotropy or quasi-periodic flow (for steady state cases) (Zaretsky, 2014). For these reasons, LES equations were utilized to evaluate the time-dependent flow characteristics in the wall-bounded flow through a CANDU fuel bundle.

4.1 Governing Equations

The LES method presumes a threshold length and time scale below which the structure of the turbulent eddies can be universally modelled; thus, only eddies that exist in the larger scales need to be simulated directly. This is achieved by low-pass filtering of the time-dependent partial differential equations representing continuity and momentum under isothermal conditions. The continuity and momentum equations for an incompressible isothermal fluid flow are respectively given as:

$$\frac{\partial \overline{u}_i}{\partial x_i} = 0 \tag{1}$$

$$\frac{\partial \rho \overline{u}_i}{\partial t} + \frac{\partial}{\partial x_j}\left(\rho \overline{u}_i \overline{u}_j\right) = -\frac{\partial \overline{p}}{\partial x_i} + \frac{\partial}{\partial x_j}\mu\left(\frac{\partial \overline{u}_i}{\partial x_j} + \frac{\partial \overline{u}_j}{\partial x_i}\right) - \frac{\partial \tau_{ij}}{\partial x_j} \tag{2}$$

In these equations, t is time, ρ is the fluid density, u_i is the i Cartesian component of velocity, x_i is the i^{th} component of Cartesian spatial coordinate, p is the static pressure, μ is the fluid viscosity, and τ_{ij} is the ij component of the residual stress tensor that comes about from filtering the Navier-Stokes equations. This stress tensor needs to be modelled to close the LES equations.

There are many variants of turbulence closure models that have been employed to filter and resolve the subgrid-scale (SGS) terms in the LES equations. Implicit filtering of the governing equation is applied in this study. In contrast to an explicit approach, the implicit filtered LES (I-LES) formulation does not rely on filtering schemes with a $2\Delta x$ cut-off (i.e., "energy drain"), rather the grid itself acts in concert with the spatial discretization to provide the filter. In addition, rather than employing an SGS model, implicit modelling is also applied in the present study and hinges on the concept associated with the numerical regularization of the resolved-scale numerics due to the effects of SGS fluid dynamical effects (Grinstein et al. 2011). Here, the truncation error of the discretization and the associated dispersive characteristics combine to represent the physics of the unresolved scales unlike explicit LES models using SGS models. Specifically with this method, a balance between phase speed and dissipation is constructed in a non-linear and monotonicity preserving procedure that respects the energy cascade throughout the discrete spectrum.

4.2 Solution Method

The CFD code HYDRA-TH was used in this work to solve the governing equations of conservation of mass and momentum. HYDRA-TH is a subset of the Hydra Toolkit and it provides a general-purpose capability for simulating incompressible and low-Mach number flows. This software was successfully used in a previous study of flow in a 37-element CANDU fuel bundle with an

undeformed pressure tube that compared well to MRV measurements (Piro et al. 2016b). A similar approach to that taken for the present study with a deformed pressure tube is used.

Numerical methods that "build-in" regularization, as is required for I-LES, may be found in stabilized finite element methods and some monotonicity-preserving finite volume methods (Grinstein et al. 2007). A detailed presentation of modified equation analysis and assessment of high-resolution (monotonicity-preserving) algorithms is described by Grinstein et al. (2007). A spectral analysis of the interplay between advective phase speed and dissipation for signals ranging from the integral to the grid Nyquist limit is described by Christon et al. (2004), Voth et al. (2004), and for HYDRA-TH is discussed in Christon et al. (2016). The modified equation analysis is important in defining the form of implicit SGS terms. HYDRA-TH also considers the spectral analysis that is critical in designing I-LES methods that accurately represent the grid-resolved eddies. The details of the non-linear, monotonicity-preserving advection scheme, and the associated phase speed and dissipation may be also found in the HYDRA-TH Theory Manual (Christon, 2011).

In HYDRA-TH, wall-functions are not used with an I-LES turbulence model, therefore requiring a mesh resolution down to a $y^+ \approx 1$ for near walls. Here, the "+" superscript denotes normalization by wall variables, ν and $u_\tau = (\tau_w/\rho)^{0.5}$; where, ν and u_τ are the kinematic viscosity and friction velocity, respectively. In these definitions, τ_w is the shear stress at the wall. An automatic time-step controller is used with a fixed Courant-Friedrichs-Levy (CFL) condition in order to capture the eddy-turnover time scale associated with eddies in the regions between the rods in the bundle. Preliminary computations were carried out to assess the time-scale when a statistically stationary flow is established by monitoring the volume integrated kinetic energy for the flow domain. The volume integrated kinetic energy is saturated and stabilized after 2 seconds of physical simuliation time, which indicated the starting point for the collection of turbulent statistics for the flow problem.

HYDRA-TH is based on a hybrid projection algorithm for time-dependent, incompressible viscous flow (Christon et al. 2016). This hybrid finite element/finite-volume algorithm circumvents the usual divergence stability constraints – such as checkerboard modes in the pressure – and does not require explicit treatment of pressure modes using Rhie-Chow interpolation or a pressure-stabilized Petrov-Galerkin formulation. The hybrid projection algorithm relies on the so-called co-velocity approach, where dual-edge velocities that are centered at unique faces in the grid are made divergence-free and then used for advection. Together with a high-resolution advection scheme with consistent edge-based treatment of viscous/diffusive terms, this yields a robust algorithm for incompressible flows.

Here, the second-order (in space and time) accurate projection method is used for the I-LES computations with a fixed-CFL automatic time-stepping algorithm. The construction of the high-resolution monotonicity-preserving algorithm with a second-order Trapezoidal rule in time permits an extended stability range. This permits stable, time-accurate I-LES computations with CFL values around 5-10. HYDRA-TH relies on PETSc (Balay et al. 2015), the ML preconditioner from Trilinos (Heroux et al. 2003), and Hypre (Falgout et al. 2015) for its linear solvers. In particular, Hypre's BoomerAMG is employed as a preconditioner to PETSc's CG solver for the pressure projection linear solve, while the momentum transport linear solve is performed using PETSc's FGMRES solver with PETSc's block Incomplete LU-decomposition as a preconditioner.

4.3 Computational Geometry

For the sake of consistency, the geometry of the CANDU fuel bundle used in the CFD simulations was made using the same CAD model that was used to manufacture the polyamide bundle. This model is a correct geometric representation of a CANDU 37-element fuel bundle used in the Bruce Nuclear Generating Station. The computational geometry also included the pressure tube 50 mm upstream fluid region and 150 mm downstream fluid region. For a concentric undeformed pressure tube, there would be a 0.89 mm gap between it and the bundle. In the present case, the pressure tube diameter is increased by 6% and the bundle rests on the bottom of the pressure tube.

4.4 Boundary Conditions

In the physical experiment, a large diffuser adapts the flow supply system at the inlet of the test rig containing the fuel bundle with a nozzle at the outlet. Again, the pre-conditioning system shown in Figure 3 used in the experiments was designed to produce a flat velocity profile at the inlet of the test rig, which eliminates the need of including it in the computational geometry.

The operating fluid for this particular problem is incompressible light water at atmospheric pressure and at a temperature of 21 °C. At this state, the density of water is taken to be 997.2 $kg \bullet m^{-3}$ and the dynamic viscosity is 0.00089043 $kg \bullet m^{-1} \bullet s^{-1}$ (Leung et al. 1999). The inlet was represented as a constant velocity inlet boundary condition. Since the I-LES turbulence closure was used, turbulent boundary conditions for turbulent kinetic energy and dissipation rate are not required at the inlet. At the outflow boundary, a zero gauge static pressure kept temporally constant in an area-averaged sense was prescribed. Finally, all surfaces were treated as adiabatic solid walls with a no-slip, no-penetration boundary condition.

4.5 Spatial Grid

Due to the lack of an explicit filter and explicit subgrid model in the I-LES formulations, the grid must be selected in a manner to ensure that the filtered length scales are small enough that the associated wavenumbers are well into the dissipative range of the turbulent spectrum. To this end, near wall boundary elements need to be small and uniform in order to adequately resolve the flow behaviour near the wall. However, for very complex flow geometries, the size and uniformity of the cells along the wall are difficult to maintain during mesh generation.

In this study, the y^+ values are evaluated with the Wall-Adapting Local Eddy-viscosity (WALE) model. Note that the I-LES model does not rely on a wall-normal distance value. For this reason, the WALE turbulence model, which does rely on an explicit wall-normal distance, was used only to estimate y^+ values in the near-wall regions. In addition, comparison studies have been performed comparing the Hydra I-LES methodology to explicit SGS models with wall damping behaviour (Yidong, et al., 2016). Here, the I-LES model was compared to the WALE model and produced comparable results. The average calculated y^+ value over the fuel bundle surface is close to 1 with a maximum value of 5. The spatial uniformity of the y^+ value is also of importance whereby the spatial distribution of y^+ over the fuel bundle is pretty smooth with small variations of y^+. A value of y^+ for the first grid point of the wall was used, with boundary layer region of the laminar sublayer of approximately $y^+ \approx 20$ (Chapman, 1979). It is also noted that the majority of turbulent kinetic energy dissipation occurs in length scales of the order of $y^+ \approx 12$ to 30 (Tanahashi et al. 2004; Moin et al. 1998).

The geometry of the bundle was constructed with SOLIDWORKS (SolidWords, 2015), which was then meshed with HEXPRESS/HYBRID (Numeca, 2014). The geometry was meshed with approximately 59 million cells, whereby 77% of the cells were hexahedrals, 18% were prisms, 3.6% were pyramids and 1.8% were tetrahedrals. HEXPRESS/HYBRID was chosen for its ability to automatically generate high quality hex-dominant meshes directly from CAD geometries, which proved to be very effective for such a highly complex geometry.

Figure 4 shows the computational mesh imposed on the fluid domain of the crept pressure and fuel bundle. In general, a three-layer inflation zone was generated near the walls of the fuel elements to capture the boundary layer with overall high resolution within the subchannels. Inserts are shown to magnify the mesh near areas of interest. The insert labelled *1* illustrates the mesh in the fluid region between adjacent fuel elements in the bundle. A particular area of interest is the location where the bundle rests on the pressure tube on bearing pads. This is shown in the enlarged insert labelled *2* in Figure 4 and indicates a good quality mesh. The inserts labelled *3* and *4* show the mesh at a bearing

pad location and just downstream of this location. A fine resolution mesh is required downstream of the bearing pads to capture turbulent phenomena that could be induced by the presence of the bearing pad. Note that some of the mesh elements may appear distorted in this figure due to the projection of a three-dimensional mesh onto a two-dimensional plane.

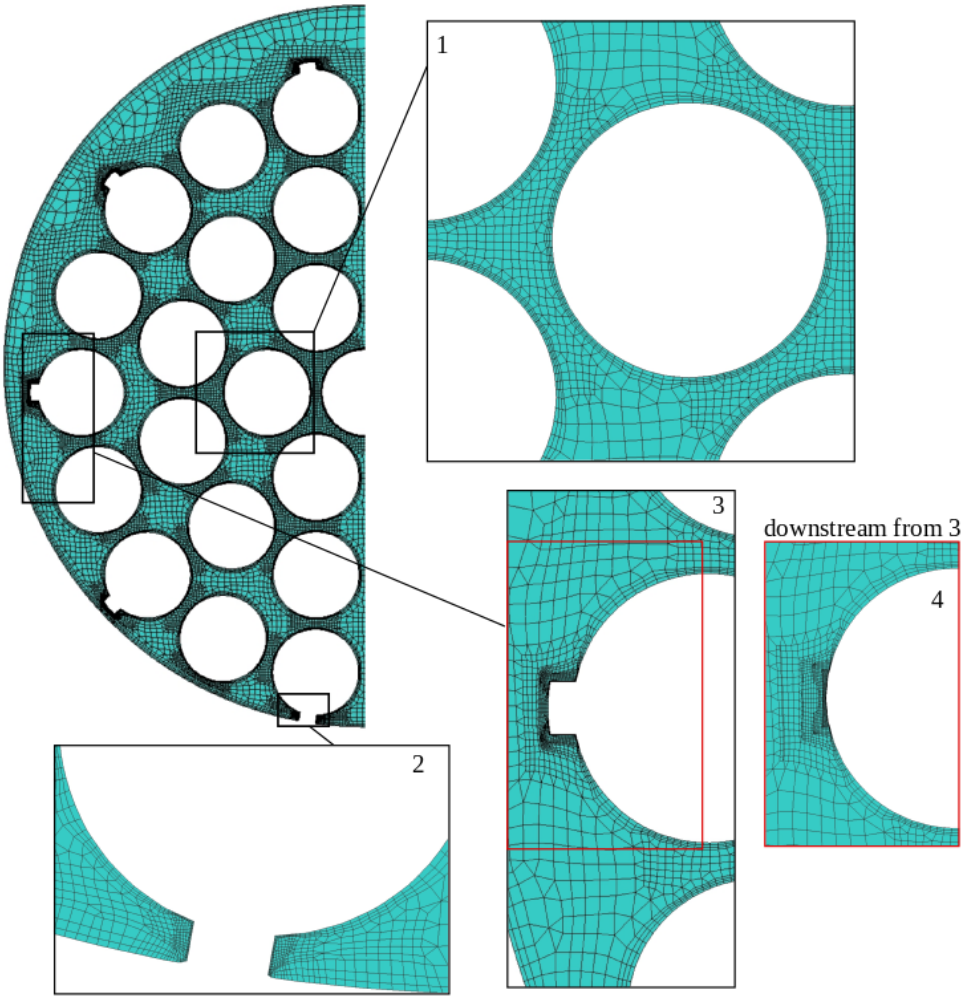

Figure 4. The computational mesh representing the fluid region within the crept pressure tube is shown.

4.6 Convergence Criteria

In this study, the semi-implicit projection time-integration scheme (Christon, 2011) was used to understand the transient flow characteristic over the complex wall-bounded flow channel. The basic philosophy of the projection method is to provide a legitimate way to decouple the pressure and velocity fields, and establish an efficient computational method for transient incompressible flow simulations. Time integration was dynamically determined by HYDRA-TH to constrain the maximum CFL number to 4, which resulted in a step size of approximately 10^{-4} s for most of the simulation (see Figure 5). The domain integrated kinetic energy, $\int \frac{\rho v^2}{2} d\Omega$, was computed by HYDRA-TH with respect to time, which is also shown in Figure 5. Here, Ω denotes the volume of the fluid domain. Based on these calculations, a time of 2 s was selected as the starting point for calculating time-integrated statistics until the end of the simulation at 4.7 s. This time interval corresponded to approximately 70,000 time steps. The initial 2 s corresponds to approximately the region of flow transition, after then, the volume-integrated kinetic energy has reached a statistically stationary state. Convergence at the time step level was determined by ensuring that the residuals of all three-momentum equations and the continuity equation were less than 10^{-5}. In addition, the outlet flow rate was monitored to ensure that continuity of the CFD domain was satisfied as the simulation progressed.

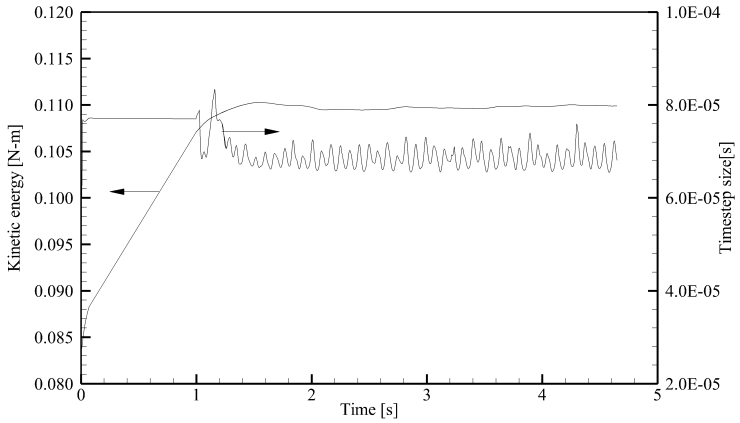

Figure 5. The computed volume-integrated kinetic energy and time step size is plotted with respect to simulation time.

5 RESULTS

The space between neighbouring fuel elements in a CANDU fuel bundle is termed a subchannel, through which the coolant is flowing. For good convective heat transfer, highly turbulent, thin boundary layers and a high fluid velocity are advantageous. Inter-subchannel mixing improves the homogenization of coolant temperature within a CANDU fuel bundle, thus promoting the normalization of fuel element temperatures.

The lack of wall-function and implicit modelling of the sub-grid scales for the I-LES method employed here means that a mesh that is too coarse would be overly dissipative. The adequacy of the computational assumptions used is qualified through comparison of the time-averaged axial velocity U_z obtained from the I-LES simulations with those of the MRV measurements. The distribution of U_z is considered for different axial positions shown in Figure 6 through the contour plots in Figure 7. In sequential order: just downstream from the bundle leading edge (z = 10 mm); downstream from the first set of bearing pads (z = 50 mm); at a flow region with aligned bearing pads (z = 250 mm); at a region of the flow with the least flow obstructions (z = 350 mm); at a flow region with staggered bearing pads (z = 400 mm); and at the outflow from the bundle (z = 494 mm). In Figure 7, the velocity is normalized by the time- and spatially-averaged inlet velocity to account for small differences in the flowrates at the inflow of the simulation and experiment.

At the axial location 10 mm downstream from the leading edge of the fuel bundle, the LES and MRV trends compare very well qualitatively. However, the simulation predicts a higher degree of reverse flow induced by larger-scale turbulence eddies created as the relatively uniform bulk fluid begins to navigate through the bundle. This deviation is expected as it is noted that just downstream of the bundle's leading edge, where the flow undergoes a high degree of acceleration, there is an inherent larger uncertainty from the MRV acquisition method [Bruschewski et al. 2016]. At 50 mm downstream of the bundle's leading edge, the contours of the simulations and experiments compare favourably. At this stage of flow development, the flow is being redistributed away from the bundle and towards the larger crevice at the top of the channel due to the crept pressure tube. As the contours at 250 mm to 400 mm indicate, much of this radial redistribution of the flow has occurred (more so in the MRV data) and a large percentage of the flow by-passes the bundle. The contours at the location of the downstream end plate are comparable, with similar degrees of reverse flow in both the measurement and simulation. The favourable comparison between the MRV and CFD data validate the numerical approach taken and confirm that the grid is sufficient to use I-LES without explicit wall functions.

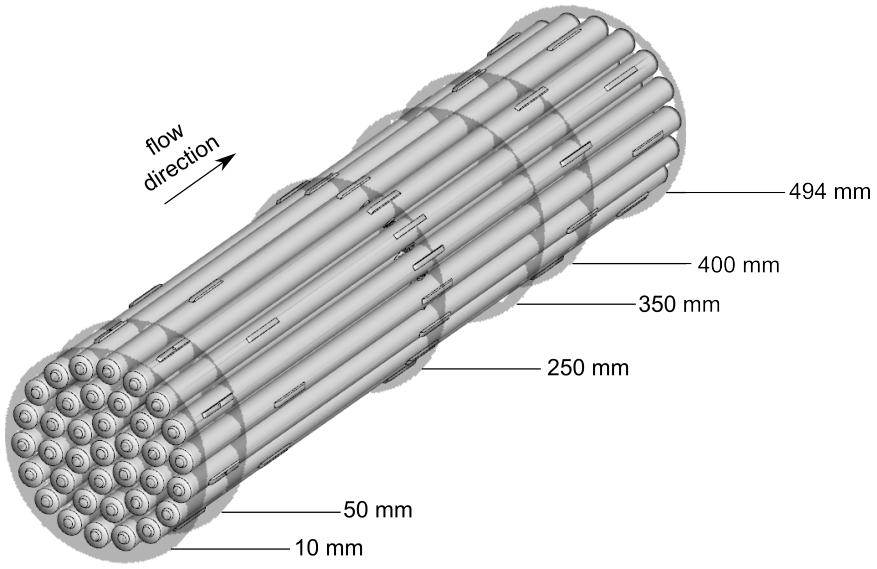

Figure 6. Virtual planes are superimposed on a 37-element fuel bundle, which indicate the locations of contour plots that compare MRV measurements and CFD simulations in Figure 7.

Figure 8 quantifies the relative amount of fluid travelling through the fuel bundle (highlighted in red) with respect to the entire fuel channel. Equivalently, this figure quantifies the amount of fluid by-passing the fuel bundle as a function of the axial distance. A value of near unity is shown near the upstream end plate since the flow is fairly uniform in this region. As to be expected, this value decreases downstream as a relatively greater portion of fluid travels through the upper region of the fuel channel. Three spikes are observed near Z = 0 mm, 250 mm and 500 mm that correspond to the upstream end plate, middle appendages, and downstream end plate, respectively. These spikes likely result from experimental errors, including partial volume effects, spatial encoding and velocity encoding errors. The discussion of these errors is provided in Bruschewski et al. (2016).

An important observation in Figure 8 is that the relative volumetric flow rate stabilizes near the end of the bundle. Since a fuel channel in a commercial reactor has 12-13 consecutive bundles, this observation implies that the flow is more or less fully developed by the end of the first bundle and the by-passing effect does not worsen. Nevertheless, these measurements demonstrate that ≈30% of the fluid by-passes the fuel bundle in a pressure tube that has experienced 6% diametral creep under the specific conditions examined herein. Again, these analyses applied a flow rate that is much less than what is experienced in-reactor. Future research should investigate flow conditions that are more representative of in-reactor conditions. Having the ability to quantify the distribution of fluid flow through a fuel bundle sitting in a crept pressure tube is important to understand the coolability of a fuel bundle. Furthermore, these analyses provide important data to support the degree of reactor de-rating, which may otherwise be overly conservative.

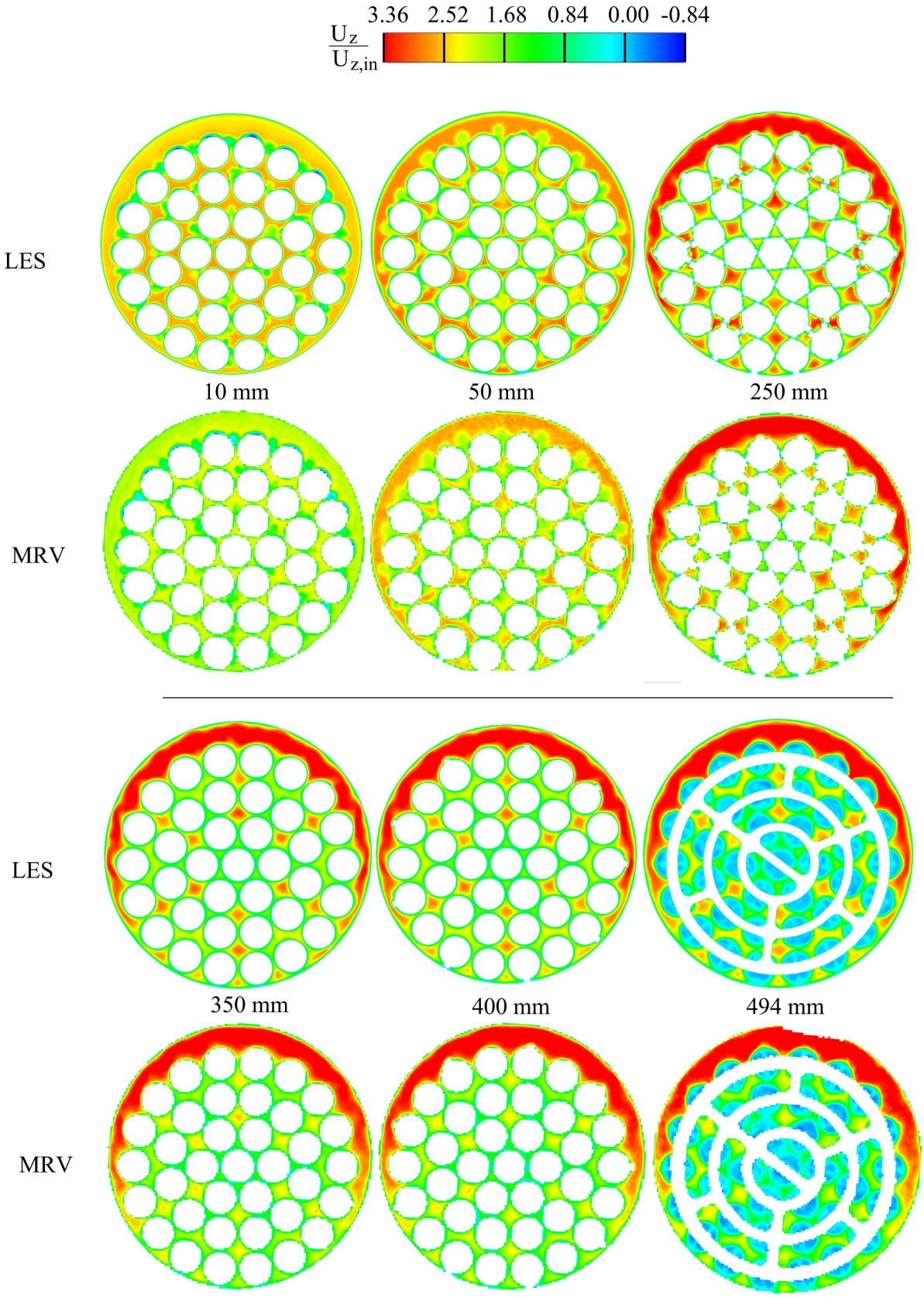

Figure 7. Contour plots compare predicted (LES) axial velocities to measured (MRV) values at various axial positions.

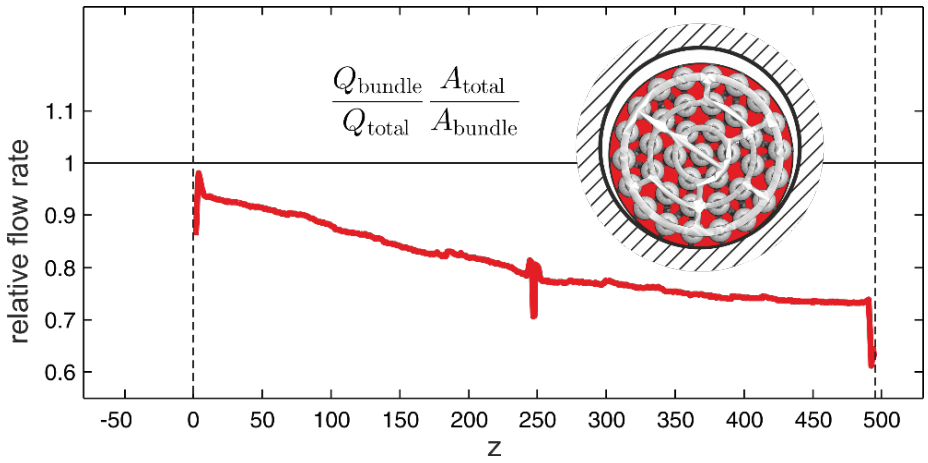

Figure 8. The above figure plots the dimensionless volumetric flow rate through the fuel bundle relative to the total flow rate. The horizontal axis represents axial distance, whereby Z = 0 mm corresponds to the middle of the upstream end plate.

6 CONCLUSIONS

Experimental and computational analyses have been presented of three dimensional, three component velocity distributions of water flowing through a 37-element CANDU fuel bundle replica sitting in a 6% crept pressure tube replica. The impetus of this work was to better understand and quantify the effects of flow by-pass, whereby coolant water preferentially passes above the fuel bundle. MRV measurements demonstrated that up to ≈30% of the fluid by-passes the bundle under these conditions. In parallel, CFD simulations were performed and generally agreed with MRV measurements, which validates the approach and gives credence to applying this simulation framework to future problems. While the temperature and pressure of the fluid investigated in this work are not fully represenative of in-reactor conditions, significant progress has been made in developing experimental and computational capabilities to investigate fluid flow through a CANDU fuel channel in high spatial detail to support nuclear reactor safety.

ACKNOWLEDGEMENTS

The authors thank N. Lair (CNL) for assistance in drafting engineering drawings and preparing figures, and Y. Liu (CNL) for assistance in using the Wukong computer cluster.

REFERENCES

F. Abbasian, S.D. Yu and J. Cao, “Experimental and Numerical Investigations of Three-Dimensional Turbulent Flow of Water Surrounding a CANDU Simulation Fuel Bundle Structure Inside a Channel”, *Nuclear Engineering and Design*, 239 (2009) 2224–2235.

S. Balay, S. Abhyankar, M. Adams, J. Brown, P. Brune, K. Buschelman, L. Dalcin, V. Eijkhout, W. Gropp, D. Karpeyev, D. Kaushik, M. Knepley, L. Curfman McInnes, K. Rupp, B. Smith, S. Zampini and H. Zhang, “PETSc User Manual”, Argonne National Laboratory, Technical Report ANL-95/11 Rev 3.6 (2015).

A. Bhattacharya, S.D. Yu and G. Kawall, “Numerical Simulation of Turbulent Flow Through a 37-Element CANDU Fuel Bundle”, *Annals of Nuclear Energy*, 40 (2012) 87–105.

M. Bruschewski, D. Freudenhammer, M.H.A. Piro, C. Tropea and S. Grundmann, “New Insights Into The Flow Inside CANDU Fuel Bundles Using Magnetic Resonance Velocimetry”, *Proc. Comp. Fluid Dyn. Nucl. React. Safety*, Cambridge, USA (2016).

D.R. Chapman, "Computational Aerodynamics Development and Outlook", AIAA Journal, 17 (197) 1283-1313.

M.A. Christon, M.J. Martinez and T.E. Voth, "Generalized Fourier Analysis of the Advection-Diffusion Equation – Part I: One-Dimensional Domains", *Inter. J. Num. Meth. Fluids*, 45 (2004) 839-887.

M.A. Christon, "Hydra-TH Theory Manual", In Tech. Rep. LA-UR 11-05387, Los Alamos National Laboratory (2011).

M.A. Christon, J. Bakosi, B.T. Nadiga and M. Berndt, M.M. Francois, A.K. Stagg, Y. Xia, H. Luo, "A Hybrid Incremental Projection Method for Thermal-Hydraulics Applications", *J. Comp. Phys.*, accepted (2016).

R. Falgout, A. Cleary, J. Jones, E. Chow, V. Henson, C. Baldwin, P. Brown, P. Vassilevski and U. Meier Yang, "Hypre User's Manual", Lawrence Livermore National Laboratory (2015).

F.F. Grinstein, L.G. Margolin and W. Rider, *Implicit Large Eddy Simulation: Computing Turbulent Fluid Dynamics*, Cambridge University Press, 2007.

M.A. Heroux and J.M. Willenbring, "Trilinos Users Guide", Sandia National Laboratories, Technical Report SAND2003-295 (2003).

R.A. Holt, "In-reactor deformation of cold-worked Zr-2.5Nb pressure tubes", *Journal of Nuclear Materials*, 372 (2008) 182-214.

L.K.H. Leung, K.F. Rudzinski, B. Verma, D.C. Groeneveld and A. Vasic, "Thermalhydraulics Evaluation Package (TEP V3.0) – A User-friendly Software Package for Evaluating Thermalhydraulics Parameters in Tubes and Bundles", Proceedings of the 9th International Topical Meeting on Nuclear Reactor Thermalhydraulics (NURETH), San Francisco, USA (1999).

P. Moin and L. Mahesh, "Direct numerical simulation: a tool in turbulence research", *Annual Review of Fluid Mechanics*, 30 (1998) 539-578.

Numeca Inter., HEXPRESS/Hybrid User Manual, Version 11 (2014).

M.H.A. Piro, F. Wassermann, S. Grundmann, B.W. Leitch and C. Tropea, "Progress in On-Going Experimental and Computational Investigations within a CANDU Fuel Channel", *Nuclear Engineering and Design*, 299 (2016) 184-200.

M.H.A. Piro, F. Wassermann, S. Grundmann, S.J. Kim, M. Christon, M. Berndt, M. Nishimura and C. Tropea, "Fluid Flow Investigations within a 37 Element CANDU Fuel Bundle Supported by Magnetic Resonance Velocimetry and Computational Fluid Dynamics", *Inter. J. Heat Fluid Flow*, in review (2016).

SolidWorks Corporation, "SolidWorks User's Guide", (2015).

M. Tanahashi, M. Kang, S.J. Miyamoto, T. Shiokawa and T, Miyauchi, "Scaling law of the fine scale eddies in turbulent channel flows up to Re_τ=800", *Inter. J. Heat and Fluid Flow*, 25 (2004) 331-340.

T.E. Voth, M.J. Martinez and M.A. Christon, "Generalized Fourier Analysis of the Advection-Diffusion Equation – Part II: Two-Dimensional Domains", *Inter. J. Num. Meth. Fluids*, 45 (2004) 889–920.

Y. Xia, C. Wang, H. Luo, M. Christon, J. Bakosi, "Assessment of a Hybrid Finite Volume and Finite Element Code for Turbulent Incompressible Flows", *J. Comp. Phys.*, 307 (2016) 653-669

A. Zaretsky, "Simulation of Intersubchannel Mixing in a Triangular Nuclear Fuel Bundle Geometry", MSc. Thesis, McMaster University, Hamilton, ON, Canada (2014).